ACS Sustainable Chemistry & Engineering

Research Article

pubs.acs.org/journal/ascecg

Hybrid Clay: A New Highly Efficient Adsorbent for Water Treatment

Emmanuel I. Unuabonah,*[,†,‡] Christina Günter,[§] Jens Weber,[∥] Susanne Lubahn,[‡] and Andreas Taubert[‡]

[†]Department of Chemical Sciences, Redeemer's University, 110115, Mowe, Nigeria

[‡]Institute of Chemistry, University of Potsdam, D-14476 Potsdam, Germany

[§]Department of Earth and Environmental Science, University of Potsdam, D-14476 Potsdam, Germany

[∥]Max Planck Institute of Colloids and Interfaces, D-14476 Potsdam, Germany

Supporting Information

ABSTRACT: New hybrid clay adsorbent based on kaolinite clay and *Carica papaya* seeds with improved cation exchange capacity (CEC), rate of heavy metal ion uptake, and adsorption capacity for heavy metal ions were prepared. The CEC of the new material is ca. 75 meq/100 g in spite of the unexpectedly low surface area (≈9 m^2/g). Accordingly, the average particle size of the hybrid clay adsorbent decreased from over 200 to 100 μm. The hybrid clay adsorbent is a highly efficient adsorbent for heavy metals. With an initial metal concentration of 1 mg/L, the hybrid clay adsorbent reduces the Cd^{2+}, Ni^{2+}, and Pb^{2+} concentration in aqueous solution to ≤4, ≤7, and ≤20 μg/L, respectively, from the first minute to over 300 min using a fixed bed containing 2 g of adsorbent and a flow rate of ≈7 mL/min. These values are (with the exception of Pb^{2+}) in line with the WHO permissible limits for heavy metal ions. In a cocktail solution of Cd^{2+}, and Ni^{2+}, the hybrid clay shows a reduced rate of uptake but an increased adsorption capacity. The CEC data suggest that the adsorption of Pb^{2+}, Cd^{2+}, and Ni^{2+} on the hybrid clay adsorbent is essentially due to ion exchange. This hybrid clay adsorbent is prepared from materials that are abundant and by a simple means that is sustainable, easily recovered from aqueous solution, nonbiodegradable (unlike numerous biosorbent), and easily regenerated and is a highly efficient alternative to activated carbon for water treatment.

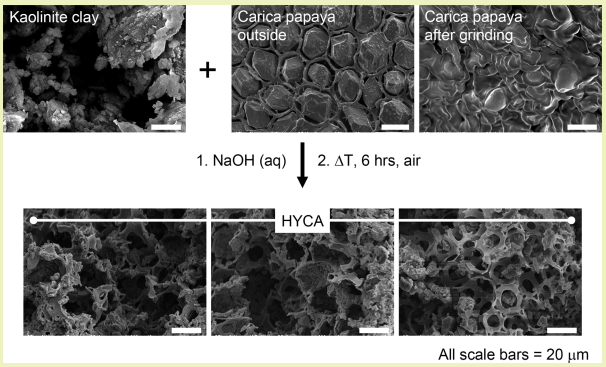

KEYWORDS: *Kaolinite, Hybrid clay, Water treatment, Cation exchange Capacity, Adsorbent, Kinetics*

INTRODUCTION

Water covers approximately 70% of the earth's surface, but less than 1% is available as freshwater for use by mankind. In many places in the world, freshwater is polluted by micropollutants, which are harmful to humans. This is particularly dramatic in the developing world, where rapidly growing industrialization (accompanied by indiscriminate release of chemical waste into the environment), increased population, and unregulated urbanization have heavily contributed to severe pollution of water and soils. As a result, over 70% of the illnesses in developing countries are related to water contamination, with a particular impact on women and children.[1]

Many industrial processes release heavy metal ions. To name a few examples, the tanning, steel, and photographic industries release Cr^{3+}, and the lead battery, paint production, and gold mining industries release Pb^{2+}.[2,3] Cadmium is released from corrosion of galvanized pipes and discharge from metal refineries as well as lead battery production.[4] Hydroelectric, mining, pulp and paper industries, incineration of municipal and medical waste, and coal-fired power plants discharge considerable amounts of Hg^{2+}.[5,6] Production of austenitic stainless steel, super alloys, nonferrous alloys, steel alloys, rechargeable batteries, catalysts, etc. discharge Ni^{2+} in significant quantities.[7] Finally, lead from automobile fumes significantly contributes to surface water contamination after being washed into water bodies by rainwater.[5]

Metal toxicity has been implicated as a major cause of many serious illnesses such as kidney damage, anemia, fatigue, musculoskeletal disorders, mood disturbances, neurological problems, high blood pressure, kidney and liver dysfunction, gastrointestinal (GI) and endocrine problems, and immune system dysfunction.[7] Lead causes learning disabilities and neurological problems in children, while cadmium and mercury cause kidney damage. Chronic genotoxicity from chromium induces gene mutations, and nickel can induce problems such as nasopharynx, lung and dermatological diseases, and malignant tumors.[8] In other words, heavy metal toxicity causes a systemic, biochemical maladaptation of the body in many different ways, and there is thus a clear need for clean water in the developing countries.

Nowadays, a number of technologies are available to purify water (with varying degree of success). These include coagulation,[9] foam flotation,[10] filtration,[11] ion exchange,[12] aerobic and anaerobic treatment,[13,14] advanced oxidation

Received: February 18, 2013
Revised: April 26, 2013
Published: May 9, 2013

processes,[15] solvent extraction,[16] adsorption,[17] electrolysis,[3] microbial reduction,[2] and activated sludge.[18] However, most of them are far too expensive for most developing countries, and their use is therefore restricted because of cost factors overriding the importance of pollution control.

Of the above techniques, adsorption is now strongly favored over the others because of its simplicity, cost effectiveness, ease of operation, and good efficiency in the physical treatment of water. Conventional adsorbents are activated carbons, zeolites, and silica gels. However, these adsorbents are again expensive and are thus shunned by industries, especially in the developing world. The past decade has therefore seen scientists—especially from the developing world—in desperate search of low-cost high volume adsorbents to replace these expensive conventional adsorbents.

There are indeed examples of low-cost adsorbents prepared from clays, agricultural, industrial, and municipal waste. The majority of these reports are on clays and agricultural waste; these appear to be the most abundant raw materials available. In spite of their very attractive adsorption properties, it is still very difficult to utilize these adsorbents on industrial scales for reasons like clogging, difficulty in recovery from industrial sieves, very low flow rates (≈2 mL/min) for clays[18] in fixed bed columns, inefficiency in removal of very low heavy metal concentrations from aqueous solutions, "bleeding", and/or decomposition of the sorbent when left in aqueous solution for some time.[19] Indeed, there are very few examples avoiding these problems so far. For example, we prepared a polymer−clay composite with very good adsorption capacity for Pb^{2+} and Cd^{2+} that circumvents the problem of recovery of clays from filters.[20−22] Though the polymer−clay composite possess a very good adsorption capacity for heavy metal ions, it is not able to reduce heavy metal ion concentrations to the microgram per liter limit, and its rate of uptake is poor.[21,22]

Recently, we reported the use of defatted *Carica papaya* seeds for the removal of methylene blue, Pb^{2+}, and Cd^{2+} from aqueous solution. The results suggest an unusually high adsorption capacity of the defatted seeds for these micropollutants.[23,24] However, the adsorbent has the usual problem of "bleeding" in columns as a result of decomposition after a few days in aqueous solution and low density. There is thus a need to further stabilize the adsorbent, while maintaining its favorable adsorption capacity.

In the world today, *Carica papaya* (*Carica papaya* L.) production ranks tenth among all fruit species grown for commercial purpose. This is closely followed by citrus (*Citrus* spp.), bananas (*Musa* spp.), grapes (*Vitis* spp.), apples (*Malus* spp.), mangoes (*Mangifera indica* L.), pineapples (*Ananas comosus Merr.*), pears (*Pyrus* spp.), and peaches (*Prunus* spp.).[25] In 2010, global production was estimated to reach 11.22 million metric tons.[26] Nigeria was ranked among other countries like Mexico, Brazil, Indonesia, and India, as a world leading *Carica papaya* producer.[26]

This study reports the successful combination of *Carica papaya* seeds (with very high adsorption capacity and kinetic rate of uptake) and kaolinite clay (with good density) without the traditional use of nitrogen atmosphere during material preparation. The resulting hybrid adsorbent is stable, easily recovered from aqueous solution via decantation, nonbleeding (does not biodegrade), cheap, and easily available in large amounts, with a high adsorption capacity for the removal of very low concentrations of Pb^{2+}, Cd^{2+}, and Ni^{2+} from aqueous solutions.

MATERIALS AND METHODS

Materials. Raw kaolinite clay was obtained from Redemption City, Mowe, Ogun State, Nigeria. After collection, stones and other heavy particles were removed from the sample. The sample was purified according to reported protocols.[27] *Carica papaya* seeds sourced from several open markets in Nigeria were sun dried until all fleshy part of the fruit was dried off the seed. The seeds were then collected into an airtight container. NaOH, $Pb(NO_3)_2$, $Cd(NO_3)_2.4H_2O$, and $NiCl_2.6H_2O$ (Merck) were used as purchased.

Hybrid Clay Adsorbent Synthesis. Equal weights (10 g each) of purified clay and dried papaya seeds were weighed into a 500 mL beaker with 200 mL of 0.1 M NaOH and stirred. The mixture was left standing for 3 days with intermittent stirring after which it was transferred into an oven and heated at 105 °C until the samples were dry. Samples of the dried mixture were weighed into crucibles and calcined at 300 °C for 6 h in air. The resulting dark powdery material was washed several times with Millipore water to remove residual NaOH from the surface of the composite and subsequently dried to remove all moisture. The dried samples were stored in an airtight container and are subsequently referred to as hybrid clay adsorbent (HYCA).

Characterization of Materials. X-ray diffraction patterns were recorded on a Siemens D-5000 from 3.0 to 70° 2θ at 0.02° s^{-1}. Scanning electron microscopy (SEM) was done on a JEOL JSM 6510 SEM equipped with an EDX spectrometer of Oxford (INCAx-act SN detector). Particle size analysis was done with a Beckman Coulter LS 230 Laser Granulometer Counter. X-ray fluorescence (XRF) data were acquired on a Bruker AXS S4 Pioneer XRF spectrometer with analysis range from Be to U. Point of zero charge (PZC) determination was done according to Kinniburgh et al.[28] Surface area determination was done on an AS1MP and a Quadrasorb machine (both of Quantachrome Instruments, Boynton Beach, FL, U.S.A.). The samples were degassed under high vacuum at 150 °C for 20 h prior to analysis. Surface areas were calculated either by the multipoint or single point Brunauer−Emmett−Teller (BET) models. Cation exchange capacity (CEC) was obtained using the ammonium acetate method in which 1 g of the material was added to 20 mL of 1 M ammonium acetate solution (pH 7.0). The mixture was agitated for 2 h. The mixture was then centrifuged, and the supernatant kept for inductively coupled plasma-atomic emission spectrometry (ICP-AES) analysis of Na^+, K^+, Ca^{2+}, and Mg^{2+}. The calculation for exchangeable bases was done using the ammonium acetate method

$$\text{Exch. Ca} = \frac{(a-b)\times 20\times \text{mcf}}{10\times 20.04\times s}$$

$$\text{Exch.Mg} = \frac{(a-b)\times 20\times \text{mcf}}{10\times 12.15\times s}$$

$$\text{Exch. K} = \frac{(a-b)\times 20\times \text{mcf}}{10\times 39.1\times s}$$

$$\text{Exch. Na} = \frac{(a-b)\times 20\times \text{mcf}}{10\times 23.0\times s}$$

where a = concentration of Ca, Mg, K, and Na (mg/L) from extract solution; b = mg/L of Ca, Mg, K and Na (mg/L) in blank solution; s = weight of sample (g); mcf = moisture correction factor; and 20 mL = column of NH_4OAc used.

Atomic weights of Ca, Mg, K, and Na are 40.078, 24.305, 39.098, 22.99 g/mol, respectively. The moisture correction factor was obtained by taking the ratio of HYCA exposed to air for 48 h and the constant dry weight of HYCA (105 °C). The summation of the exchangeable cations (Ca^{2+}, Mg^{2+}, Na^+, and K^+) gives the cation exchange capacity (CEC).

Adsorption/Desorption of Micropollutants. A fixed weight of HYCA adsorbent (1 or 2 g) was added to a 30 cm × 6 cm glass column. The filled columns were flushed with 20 mL of water to wash off residual carbon from the surface. With the column delivering clean and clear deionized water and with the deionized water allowed to run

out completely, solutions with known metal salt concentrations (Pb, Ni, Cd, 1−10 mg/L) at pH 5.0 ± 0.15 were added. The flow rate of the column was ca. 7 mL/min. Effluents from the column were collected at selected time intervals and analyzed using ICP-AES. The spent HYCA was regenerated using 0.1 M HNO_3.

THOMAS MODEL

The Thomas model is widely used in column performance modeling. Its derivation assumes Langmuir kinetics of adsorption−desorption and no axial dispersion so that the driving force for adsorption obeys second-order reversible reaction kinetics. The expression for the Thomas model[29] for adsorption in a fixed bed is given as

$$\frac{C_t}{C_0} = \frac{1}{1 + \exp[(k_{Th}q_e x/Q) - k_{Th}C_0 t)]} \quad (1)$$

where k_{Th} (mL min^{-1} mg^{-1}) is the kinetic coefficient; x is the total dry weight of the adsorbent (g); t is time (min); C_t is the concentration of adsorbate per time (mg L^{-1}); C_0 is the initial concentration of adsorbate (mg L^{-1}); Q is the flow rate (mL/min); and q_e (mg g^{-1}) is the predicted adsorption capacity. All breakthrough plots were made using KyPlot version 2.0 software.

RESULTS AND DISCUSSIONS

Physicochemical Analysis. *Fourier Transform Infrared Spectroscopy and X-ray Diffraction.* Figure 1 shows representative X-ray diffraction (XRD) patterns and infrared (IR) spectra of the raw materials and the HYCA. IR spectra of the *Carica papaya* material exhibit a broad but very strong −OH peak at 3402 cm^{-1} indicating the presence of phenolics and/or carboxylic −OH stretching vibrations.[30] The broad band between 3480 and 3440 cm^{-1} is an −N−H stretching vibration associated with a N-substituted amide.[30] The medium absorption bands at 2930 and 2380 cm^{-1} are the −C−H (for methyl and methylene) and =N−H$^+$ stretching vibrations, respectively.[31] A distinct absorption band at 1650 cm^{-1} is associated with a C═O stretching vibration. A peak around 1040 cm^{-1} suggests an −S═O vibration.[31,32] The spectra of the raw clay exhibit a band at 3620 cm^{-1}, which suggests the presence of inner hydroxyl groups (−OH stretching vibration) lying between the tetrahedral and octahedral sheets in the kaolinite clay mineral with a vector orientation near to the (001) plane (pointed in the direction of the vacant octahedral site).[33,34] The other three peaks (3697, 3670, and 3649 cm^{-1}) are −OH groups residing at the octahedral surface of the layers that form weak hydrogen bonds with oxygens of the Si−O−Si bonds on the lower surface of the next layer. The 3697 and 3670 cm^{-1} peaks are related to bands that are the coupled antisymmetric and symmetric vibrations of −OH,[35,36] while the weak absorption band at 3649 cm^{-1} has been suggested to be due to a symmetry reduction from an inner surface hydroxyl.[37] The bands observed at 3437 and 1630 cm^{-1} are H−O−H stretching and bending vibrations of absorbed water.[38] The absorption peak at 1626 cm^{-1} is an −OH bending vibration from absorbed water.[39] The small peaks in the 1300−400 cm^{-1} range confirm the presence of Si−O stretching and bending as well as −OH bending vibrations. Bands at 1070 and 910 cm^{-1} correspond to the Si−O and Al−OH in plane bending vibrations, respectively.[40] The Al−O− bending vibration of kaolinite was observed at 912 cm^{-1}. The doublet at 779 and 796 cm^{-1} is due to Si−O−Si inter-tetrahedral bridging bonds in SiO_2 and −OH deformation band of gibbsite.[40] IR spectroscopy therefore confirms that the inorganic material essentially consists of kaolinite.

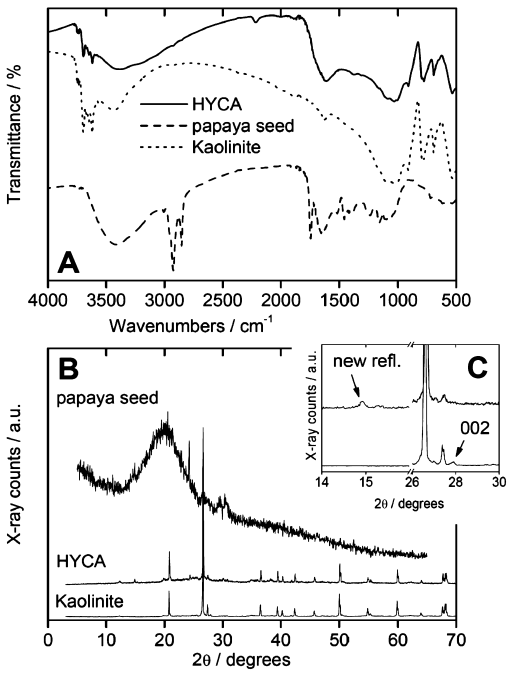

Figure 1. (A) FTIR spectra and (B) XRD patterns of pure kaolinite clay, pure, dried papaya seeds, and HYCA. Panel (C) is a magnified view of the reflections mentioned in the text. The labels "002" and "new refl." refer to the kaolinite 002 reflection and the new reflection appearing after HYCA synthesis, respectively.

For the HYCA adsorbent, the 1047 cm^{-1} Si−O bending vibration shows a significant shift when compared to the raw clay. This suggests that this position is perhaps one of the active sites for interaction of the kaolinite with the *Carica papaya* seeds. An amine −N−H band was observed in the composite spectrum at 1616 cm^{-1} with a characteristic weak −C−N band at 1394 cm^{-1}. The other bands are identical to those of the kaolinite clay.[31,41] Overall, IR confirms that the HYCA material is indeed a composite consisting of kaolinite and organic matter arising from the papaya seeds.

The presence of kaolinite in the samples is further confirmed via XRD. The only difference between the kaolinite raw material and HYCA is the disappearance of the kaolinite (002) reflection at 27.9° 2θ and the appearance of a new reflection at 14.9° 2θ. These data suggest that the order along the crystallographic c-axis of kaolinite is disturbed by the reaction between the papaya seeds and the kaolinite. The rest of the crystal structure is not affected by the HYCA synthesis process, indicating that the crystallography of the individual clay layers is not affected.

The XRD patterns of the papaya seeds with two broad and overlapping reflections essentially indicate a low order structure. Correspondingly, the XRD patterns of the HYCA sample are noisier than those of the raw kaolinite indicating that the incorporation of *Carica papaya* seeds via heating lowers the overall long-range order in the resulting HYCA material, presumably by disturbing the interlayer geometry between individual mineral layers.

X-ray Fluorescence, PZC, BET, and Elemental Analysis. Table 1 summarizes the results obtained from X-ray fluorescence (XRF) spectroscopy. HYCA has a higher silica

Table 1. X-ray Fluorescence Analysis of Raw Kaolinite Clay, *Carica papaya* Seeds, and HYCA Adsorbent

% oxide	raw clay (%)	*Carica papaya* seed (%)	HYCA (%)
SiO_2	58.30	0.13	47.1
Al_2O_3	23.90	0.05	10.2
Na_2O	0.23	0.05	0.55
K_2O	1.40	4.18	2.00
CaO	0.21	1.11	2.67
Fe_2O_3	5.43	0.05	0.98
TiO_2	1.18	–	1.00
CuO	0.04	0.01	0.02
SO_3	0.04	1.49	0.76
BaO	0.21	–	0.01
P_2O_5	0.08	1.74	1.58
PbO	–	0.01	–
MoO_3	0.02	0.01	0.02
V_2O_5	0.01	–	–
CdO	–	0.013	–
NiO	0.02	0.004	0.01
ZrO_2	0.04	–	–
Rb_2O	0.03	–	–

to alumina ratio (4.62) than the original kaolinite (2.44) due to leaching of silicon and aluminum during base treatment (see Materials and Methods). XRF also finds a number of other elements that are typical for natural kaolinite. XRF is further confirmed by energy dispersive X-ray spectroscopy (EDX, table not shown), which also finds a number of elements typical for kaolinite (Ti, Fe, Ca, K, Si, and Al).

Elemental analysis (Table 2) clearly shows that the hybrid clay material contains a significant fraction of organic material.

Table 2. Elemental Analysis Data of Kaolinite, Papaya Seeds, and HYCA

%	kaolinite	*Carica papaya* seed	HYCA
C	0.16 ± 1.7	54.9 ± 3.6	13.7 ± 1.7
H	–	6.3 ± 1.2	0.92 ± 0.08
N	–	4.6 ± 1.1	2.8 ± 0.4
S	–	1.9 ± 0.3	–
O	–	32.3[a]	42.6[b]

[a]This amount is calculated from the difference to 100%. [b]From energy dispersive X-ray analysis.

While the original kaolinite contains below 0.2% of carbon, HYCA contains roughly 14% of carbon. HYCA also exhibits a measurable amount of H and N, an indication of a significant fraction of organic material in the material. However, the reduction in the amount of H atoms in HYCA as compared with Carica papaya seeds (Table 2) may suggests an increase in π-electrons in HYCA.

An important parameter for heavy metal ion adsorption is the charge state of the adsorbent. Although the pH of point zero charge (pH_{pzc}) is 4.98 for the pure kaolinite and approximately 7.0 for the papaya seeds and HYCA (Figure 2), the pH of HYCA adsorbent was 7.53. It was observed that adsorption of Ni^{2+}, Cd^{2+}, and Pb^{2+} was very significant below the pH_{pzc} value. It is possible that our modification of kaolinite clay with a biomass (*Carica papaya* seeds) may have formed surface oxygen groups which when ionized increase the attractive electrostatic interactions between the surface of the activated carbon and the metallic cations present. According to

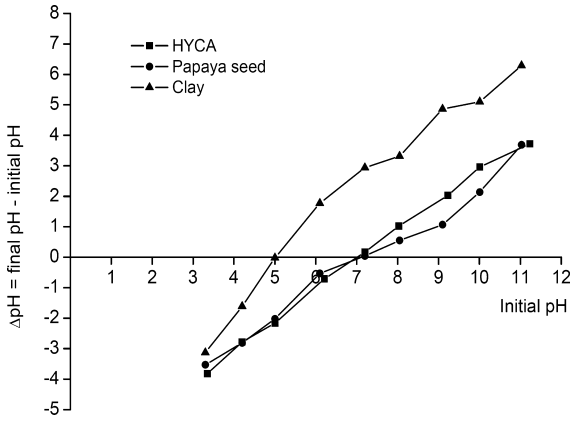

Figure 2. pH_{pzc} plot for *Carica papaya* seed, kaolinite clay, and HYCA adsorbents.

Saanchez-Polo and Rivera-Ultrilla,[42] they suggested that delocalized π electrons, responsible for the basicity of biomass materials activated via heating and chemicals, play a determinant role in the adsorption mechanism via the following equilibrium

$$-C\pi + 2H_2O \leftrightarrow -C\pi - H_3O^+ + OH^- \quad (1)$$

The basicity of HYCA adsorbent could be due to the presence of oxygen-containing functional groups (e.g., pyrones or chromenes) and/or graphene layers that act as Lewis bases and form electron donor–acceptor (EDA) complexes with H_2O molecules (eq 1).[42] The Cπ–cation interaction between the ionizable protons of surface oxygen groups and metallic cations explains the high adsorption capacity shown by HYCA adsorbent for the removal of Ni^{2+}, Cd^{2+}, and Pb^{2+} from aqueous solutions.

Figure 3 shows scanning electron microscopy images of the raw kaolinite, papaya seeds, and HYCA. The SEM images

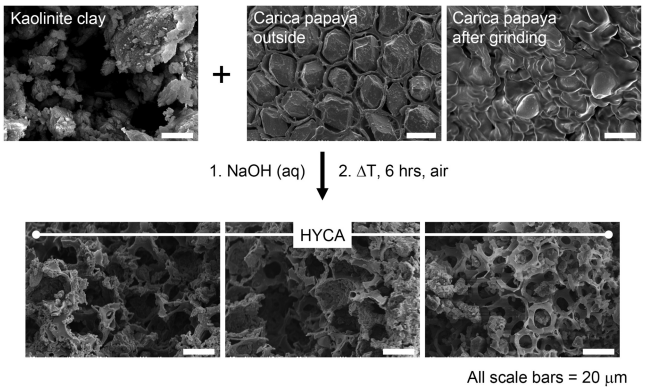

Figure 3. SEM images of the raw kaolinite, papaya seeds, and HYCA.

suggest that the HYCA adsorbent is a heterogeneous composite (Figure 3). From the images of HYCA adsorbent (Figure 3), it is observed that the clay particles have reduced sizes.

This is supported from the results of particle size analysis of the adsorbents in which kaolinite clay and *Carica papaya* seed particles sizes decreased from a mean size of 151.3 and 212.9 μm, respectively, to 100.6 μm in the HYCA adsorbent (Figure S1 a–c, Supporting Information). The HYCA adsorbent showed a very low surface area (≈9 m^2/g) similar to kaolinite clay (≈20 m^2/g) and *Carica papaya* seed (≈11 m^2/g),

dx.doi.org/10.1021/sc400051y | ACS Sustainable Chem. Eng. 2013, 1, 966–973

suggesting that the new material is not microporous or mesoporous (Figure S2a, Supporting Information). This is also confirmed from the very poor CO_2 adsorption of the material (Figure S2b, Supporting Information). The high adsorption rate (see below) could hence be due to the improved ion-exchange capacity (≈75 meq/100g) as compared with that of the kaolinite clay (2.59 meq/100g) rather than to adsorption in pore spaces.

Thermal Analysis. Thermogravimetric (TGA) and Differential Thermal Analysis (DTA). Figure 4 shows TGA and DTA

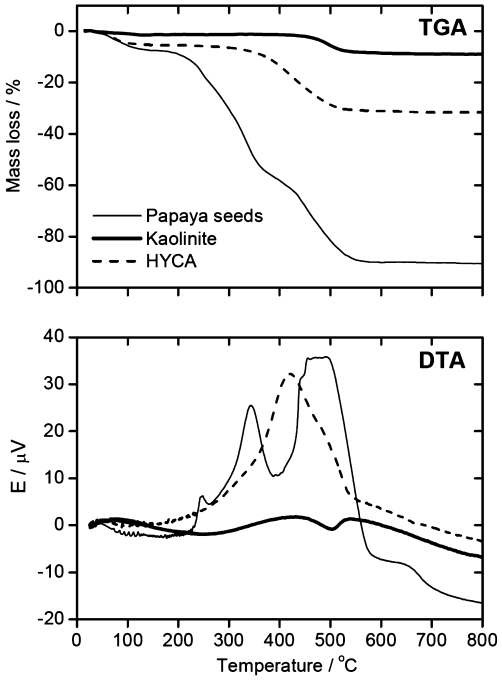

Figure 4. TGA and DTA curves for kaolinite clay, *Carica papaya* seed, and HYCA.

data of samples. TGA of kaolinite clay used in this study showed a total weight loss of 9% with the loss of interlayer water and thermal dehydroxylation process accounting for 1.3% (30−150 °C) and 7.7% (382−793 °C), respectively (Figure 4).[35,43,44] This was confirmed by DTA plots (Figure 4) that showed exothermic and endothermic peaks at 75 and 503 °C, respectively, typical of kaolinite clay. According to Frost and Vassallo,[35] the hydroxyl groups are progressively lost from 420 °C onward, and this loss is complete at 520 °C, which is in accordance with the data obtained here.

A total weight loss of 90% was observed with *Carica papaya* seeds involving three steps. The first weight loss, which is ca. 7.4% loss due to moisture, occurs between 30 and 150 °C. The second loss represents the loss of light volatiles (50%), and the third step corresponds to the loss of heavy volatiles between 400 and 540 °C. From 550 to 900 °C, two more reactions occur: the combustion of fixed carbon and the decomposition of tars.[45,46] DTA of *Carica papaya* seeds shows three exothermic peaks at a maximum of 247, 343, and 471 °C. The second and the third stages represent extended exothermal effects and mass loss, respectively. Both stages are a result of carbonization and burning of lignocelluloses in *Carica papaya* seeds.[47] There is a fourth exothermal peak maximum at 650 °C, which is an extension of the second and third stages.[47]

The high thermal reactivity and the very high rates of mass losses from *Carica papaya* seed can be attributed to the high contents of volatiles in this sample, which is a combination of hemicellulosics and cellulosics that contribute to the formation of volatiles.[48] *Carica papaya* seeds contain ≈26% carbohydrate.[49] These constituents are rich in relatively weak ether bonds and are therefore thermally unstable, enabling the formation of volatile species that are combustible.[50] Elimination of the volatiles from the solid matrix introduces pores in the residue.[51]

HYCA showed a two step degradation process in which 5.7% of the original mass (35−199 °C) was lost as adsorbed water, and 26% (200−787 °C) was lost due to dehydroxylation and devolatilization reactions. A total weight loss of ca. 32% was observed after 790 °C. A very sharp and broad exothermic peak at a maximum of 420 °C suggests that only the heavy volatiles are left in the samples after HYCA preparation because the heating process to 300 °C during HYCA preparation would have eliminated all the lighter volatiles in the material (Figure 4). This exothermic peak is largely from the *Carica papaya* seed in the hybrid material as kaolinite clay only shows weak exothermic signals between 30 and 150 °C.

Adsorption of Heavy Metal Ions. The HYCA adsorbent was used to remove Ni^{2+}, Cd^{2+}, and Pb^{2+} from aqueous solution with initial metal concentrations of 1 mg/L. After 5 h, all columns containing 2 g of HYCA adsorbent produced equilibrium solutions with concentration of Ni^{2+} at ≤7 μg/L, Cd^{2+} at ≤4 μg/L, and Pb^{2+} at ≤20 μg/L (Tables S1−S3, Supporting Information), which were the sensitivity limits of the ICP-AES instrument used for analysis. This result is in line with the WHO[52] permissible limit for heavy metal ions except for lead, which exceeded the limit by ≈5 μg/L. This could be due to the sensitivity limit of the ICP-AES used. However, with 2 g of HYCA adsorbent in the fixed bed and a cocktail of 10 mg/L each of heavy metal ion, concentrations of effluent solutions (from the fixed bed) were ≤4, ≤ 7, and ≤20 μg/L for Cd^{2+}, Ni^{2+}, and Pb^{2+}, respectively, within the first 40 min. Beyond this time, concentration of effluent solutions increased above standard limits except for Pb^{2+}, which remained at ≤20 μg/L even after 3 h. Decreasing the weight of HYCA adsorbent in the fixed to 2 g reduced both the efficiency of the adsorbent and the rate of metal ion uptake (Tables S4 and S5, Supporting Information). In the presence of toluene and benzene, the efficiency of HYCA adsorbent to keep Pb^{2+} at a ≤20 μg/L level in a cocktail solution was maintained for 1 h, while Cd^{2+} and Ni^{2+} were kept at ≤4 and ≤20 μg/L levels within the first 10 and 1 min, respectively (Table S6, Supporting Information). This suggests that the HYCA adsorbent has a stronger preference for Pb^{2+} than for Cd^{2+} and Ni^{2+} in a multimetal ion system but is strongly affected by the presence of nonionic organic contaminants.

Apparently, HYCA adsorbs organic impurities due to its carbon content, which should provide good surface adsorption sites for nonpolar organics like benzene and toluene via $\pi-\pi$ interaction. This co-adsorption might enhance the hydrophobicity of the HYCA, which could result in a strong rejection of Cd^{2+} and Ni^{2+} (hydration energy: 1807 and 2106 kJ/mol, respectively).[53] These hydration energies are higher than the one of Pb^{2+} (1481 kJ/mol), i.e., Cd^{2+} and Ni^{2+} do not lose their hydration shell easily. As the hydrophobicity of the surface is enhanced, their adsorption is reduced compared to Pb^{2+}, which can handle the more hydrophobic surface more easily. This strongly suggests that HYCA may find very good use in the co-

removal of organic contaminants and Pb^{2+} from aqueous solution.

Kinetic Study. Figure 5 shows Thomas model plots for the adsorption of Ni^{2+}, Cd^{2+}, and Pb^{2+} onto HYCA. Note that 2 g

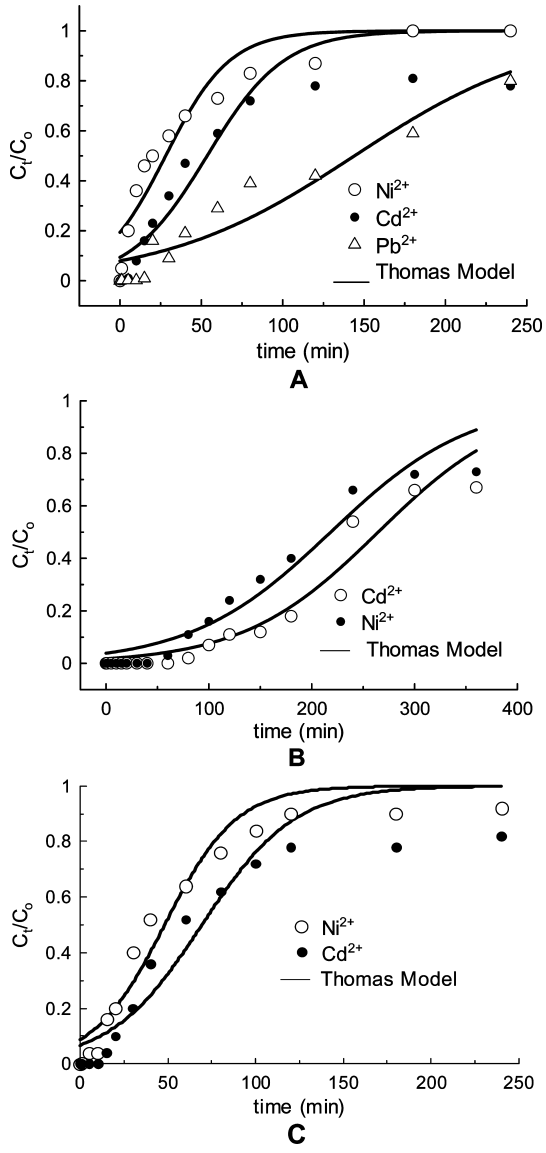

Figure 5. Breakthrough curves for the adsorption of Ni^{2+}, Cd^{2+}, and Pb^{2+} onto (A) 1 g HYCA adsorbent, (B) Ni^{2+} and Cd^{2+} onto 2 g HYCA adsorbent, and (C) Ni^{2+} and Cd^{2+} onto 2 g HYCA adsorbent in the presence of toluene and benzene.

of HYCA (cocktail solution and cocktail solution with toluene and benzene) data for Pb^{2+} were difficult to obtain because the values for Pb^{2+}, as shown in Tables S5 and S6 of the Supporting Information, were either constant throughout or for a greater part of the adsorption period.

Table 3 shows kinetic data obtained from nonlinear Thomas model plots using KyPlot 2.0 software. From the adsorption capacity values (q_e) in table 3, it is clear that HYCA adsorbent shows a strong preference for Pb^{2+} than for other metal ions. The overall rate of uptake of HYCA, K_{Th}, for Pb^{2+} is however lower than that for other metal ions in a cocktail solution. The rate of uptake (K_{Th}) seems to show an inverse relationship with the amount of metal ion adsorbed at equilibrium, q_e (Table 3).

Table 3. Thomas Model Parameters for Adsorption of Ni^{2+}, Cd^{2+}, and Pb^{2+} onto HYCA Adsorbent

	K_{Th} (mL min^{-1} g^{-1})	q_e (mg g^{-1})	r^2
1 g of HYCA (cocktail solution)			
Ni^{2+}	5.08	0.98	0.9026
Cd^{2+}	4.23	1.87	0.8720
Pb^{2+}	1.70	5.04	0.9060
2 g of HYCA (cocktail solution)			
Ni^{2+}	1.47	7.65	0.9458
Cd^{2+}	1.52	9.26	0.9477
Pb^{2+}	–	–	–
2 g of HYCA (cocktail solution with toluene and benzene)			
Ni^{2+}	4.89	1.68	0.9514
Cd^{2+}	3.79	2.43	0.9065
Pb^{2+}	–	–	–

This could be explained to mean that with increasing adsorption capacity of an adsorbent you require more time to reach equilibrium and hence the lower the overall rate constant. However, adsorption capacity for Ni^{2+} and Cd^{2+} were enhanced when 2 g of the HYCA material was used. This may not suggest a synergistic effect, but it could simply mean that with increasing adsorbent dose more sites are available for the adsorption of these metal ions that reflects in the adsorption capacity of the material. There is an observed significant decrease in the adsorption capacity of HYCA adsorbent for Ni^{2+} and Cd^{2+}, respectively, when toluene and benzene are introduced into the cocktail solution of the metal ions (Table 3).

Desorption. The regenerability of HYCA was exemplified with Ni^{2+}. A 100 mg/L solution of Ni^{2+} was incubated with 2 g of HYCA to ensure that the active sites on the adsorbent are saturated. HYCA was then subsequently regenerated with 0.1 M HNO_3. The regenerated adsorbent was then used to treat Ni^{2+} solutions with metal concentrations of 1 mg/L. In a desorption experiment, 82.8% of 100 mg/L Ni^{2+} adsorbed by HYCA was released on treatment with 0.1 M HNO_3 (Figure 6). On reuse of the regenerated HYCA adsorbent to readsorbed 1 mg/L of Ni^{2+}, it was observed that there was no difference in the pattern of uptake of Ni^{2+} from aqueous solution before and after regeneration (Tables S1 and S7, Supporting Information). Although a conclusive statement cannot be made based on this desorption data, it is however

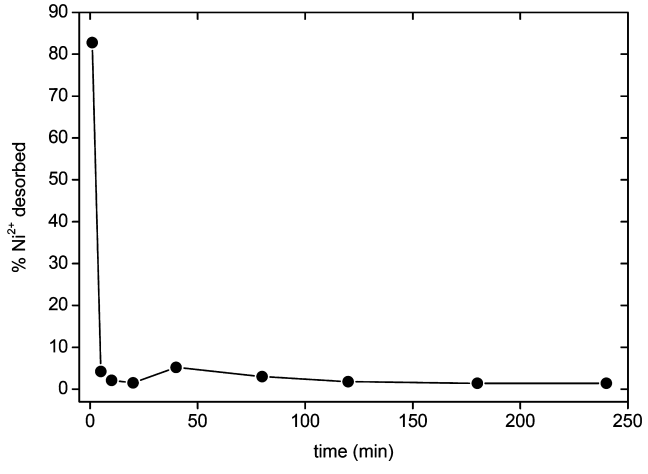

Figure 6. Desorption profile of 100 mg/L Ni^{2+} on HYCA material.

dx.doi.org/10.1021/sc400051y | ACS Sustainable Chem. Eng. 2013, 1, 966−973

clear that HYCA has the potential of being an excellent ion-exchange material and has the potential to be easily regenerated. Further studies are on to ascertain its life cycle and the best reagent for regeneration of the metal-laden HYCA adsorbent.

CONCLUSION

A low cost adsorbent was prepared without the usual nitrogen atmosphere normally used in the preparation of activated carbon. Although the surface morphology of HYCA suggests that the material is porous, surface area analysis indicates a poor surface area (≈9 m^2/g), in spite of which HYCA showed a high cation exchange capacity (≈75 meq/100 g). Further investigation showed presence of organic matter in the composite. HYCA adsorbed heavy metal ions (Pb^{2+}, Cd^{2+}, and Ni^{2+}) from 1 mg/L solutions with very high efficiency, reducing concentrations of heavy metal ions to WHO standard permissible limits except for Pb^{2+}, where instrument sensitivity was the limiting factor in analysis. Furthermore, a synergy was observed when both clay and *Carica papaya* seed were made into a composite: increased cation exchange capacity and no "bleeding" of the column when the HYCA composite adsorbent was left in aqueous solution for over 10 days as compared with *Carica papaya* seeds. The use of a non-nitrogen environment (as used in the preparation of conventional activated carbon) is a further asset for HYCA production in developing countries where provision of nitrogen gas could be a serious issue capable of hampering its production or making it cost prohibitive. This study has shown that the low cost composite adsorbent HYCA has a strong potential for replacing commercial activated carbon in treatment of wastewater in the developing world.

ASSOCIATED CONTENT

Supporting Information

Figures for particle size analysis for various materials and N_2 and CO_2 adsorption and desorption isotherms for hybrid clay adsorbent. Tables show data for the adsorption and desorption of Ni^{2+}, Cd^{2+}, and Pb^{2+} onto hybrid clay adsorbent in a fixed bed. This material is available free of charge via the Internet at http://pubs.acs.org.

AUTHOR INFORMATION

Corresponding Author

*E-mail: iyaemma@yahoo.com. Tel.: ++49 (0)331 977 5773. Fax: ++49 (0)331 977 5055.

Notes

The authors declare no competing financial interest.

ACKNOWLEDGMENTS

We thank Dr. M. Junginger and R. Löbbicke for help in the laboratory and Dr. B. Hannemann for help with EA. E.I.U. acknowledges a Georg Forster Fellowship (Alexander von Humboldt Foundation). The Max Planck Institute of Colloids and Interfaces, University of Potsdam, and Alexander von Humboldt Foundation are thanked for financial support.

REFERENCES

(1) Drinking Water: Understanding the Science and Policy Behind a Critical Resource. National Academies. www.water.nationalacademies.org (accessed October 14, 2011).

(2) Shen, H.; Wang, Y.-T. Biological reduction of chromium by *E. coli*. *J. Environ. Eng. Div. (Am. Soc. Civ. Eng.)* **1994**, *120*, 560−571.

(3) Szpyrkowicz, L.; Naumczyk, J.; Zillio-Grandi, F. Electrochemical treatment of tannery wastewater using Ti/Pt and Ti/Pt/Ir electrodes. *Water Res.* **1995**, *29*, 517−524.

(4) Duruibe, J. O.; Ogwuegbu, M. O. C.; Egwurugwu, J. N. Heavy metal pollution and human biotoxic effects. *Int. J. Phy. Sci.* **2007**, *2* (5), 112−118.

(5) Olade, M. A. Heavy Metal Pollution and the Need for Monitoring: Illustrated for Developing Countries in West Africa. In *Lead, Mercury, Cadmium and Arsenic in the Environment*; Hutchinson, T. C., Meema, K. M., Eds.; John Wiley & Sons, Inc.: Hoboken, NJ, 1987.

(6) Mercury: Time to Act; UNEP Report 2013; United Nations Environment Programme: Nairobi, Kenya, 2013. http://www.unep.org/PDF/PressReleases/Mercury_TimeToAct.pdf (accessed May 11, 2013).

(7) Bock, S. J. Diagnosis and Treatment of Heavy Metal Toxicity. http://ebookbrowse.com/di/diagnosis-and-treatment-of-heavy-metal-toxicity?pdf=on (accessed May 11, 2011).

(8) Kristiansen, J.; Christensen, J. M.; Henriksen, T.; Nielsen, N. H.; Menne, T. *Anal. Chim. Acta* **2000**, *403*, 265−272.

(9) Tan, B. H.; Teng, T. T.; Omar, A. K. M. Removal of dyes and industrial dye wastes by magnesium chloride. *Water Res.* **2000**, *34*, 597−601.

(10) Mavros, P.; Danilidou, A. C.; Lazaridis, N. K.; Stergiou, L. Color removal from aqueous solutions. Part I. Flotation. *Environ. Technol.* **1994**, *15*, 601−616.

(11) Zouboulis, A. I.; Lazaridis, N. K.; Grohmann, A. Toxic metals removal from waste waters by upflow filtration with floating filter medium. I. The case of zinc. *Sep. Sci. Technol.* **2002**, *37*, 403−416.

(12) Bolto, B.; Dixon, D.; Eldridge, R.; King, S.; Linge, K. Removal of natural organic matter by ion exchange. *Water Res.* **2002**, *36*, 5057−5065.

(13) LaPara, T. M.; Konopka, A.; Nakatsu, C. H.; Alleman, J. E. Thermophilic aerobic wastewater treatment in continuous-flow bioreactors. *J. Environ. Eng. Div. (Am. Soc. Civ. Eng.)* **2000**, *126*, 739−744.

(14) Bell, J.; Plumb, J. J.; Buckley, C. A.; Stuckey, D. C. Treatment and decolorization of dyes in an anaerobic baffled reactor. *J. Environ. Eng. Div. (Am. Soc. Civ. Eng.)* **2000**, *126*, 1026−1032.

(15) Esplugas, S.; Gimenez, J.; Contreras, S.; Pascual, E.; Rodriguez, M. Comparison of different advanced oxidation processes for phenol degradation. *Water Res.* **2002**, *36*, 1034−1042.

(16) Lin, S. H.; Juang, R. S. Removal of free and chelated Cu(II) ions from water by a nondispersive solvent extraction process. *Water Res.* **2002**, *36*, 3611−3619.

(17) Faust, S. D.; Aly, O. M. *Adsorption Process for Water Treatment*; Butterworths Publishers: Stoneham, MA, 1987.

(18) Pala, A.; Tokat, E. Color removal from cotton textile industry wastewater in an activated sludge system with various additives. *Water Res.* **2002**, *36*, 2920−2925.

(19) Demirbas, A. Heavy metal adsorption onto agro-based waste materials: A review. *J. Hazard. Mater.* **2008**, *157* (2−3), 220−229.

(20) Unuabonah, E. I.; Adebowale, K. O.; Olu-Owolabi, B. I.; Yang, L. Z. Comparison of sorption of Pb^{2+} and Cd^{2+} on kaolinite clay and polyvinyl alcohol-modified kaolinite clay. *Adsorption* **2008**, *14* (6), 791−803.

(21) Unuabonah, E. I.; El-Khaiary, M. I.; Olu-Owolabi, B. I.; Adebowale, K. O. Predicting the dynamics and performance of a polymer−clay-based composite in a fixed bed system for the removal of lead (II) ion. *Chem. Eng. Res. Des.* **2012**, *90*, 1105−1115.

(22) Unuabonah, E. I.; Olu-Owolabi, B. I.; Fasuyi, E. I.; Adebowale, K. O. Modeling of fixed-bed column studies for the adsorption of cadmium onto novel polymer−clay composite adsorbent. *J. Hazard. Mater.* **2010**, *179*, 415−423.

(23) Unuabonah, E. I.; Adie, G. U.; Onah, L. O.; Adeyemi, O. G. Multistage optimization of the adsorption of methylene blue Dye onto defatted *Carica papaya* seeds. *Chem. Eng. J.* **2009**, *155*, 567−579.

(24) Adie, G. U.; Unuabonah, E. I.; Adeyemo, A. A.; Adeyemi, O. G. Biosorptive removal of Pb^{2+} and Cd^{2+} onto novel biosorbent: Defatted carica papaya seeds. *Biomass Bioenergy* **2011**, *35* (7), 2517−2525.
(25) Morales-Payan, J. P.; Stall, W. M. Papaya (*Carica papaya*) response to foliar treatments with organic complexes of peptides and amino acids. *Proc. Florida State Hortic. Soc.* **2003**, *16*, 30−32.
(26) Statistical Database. In *FAOSTAT Statistical Yearbook 2012*; Food and Agricultural Organization of the United Nations (FAO): Rome, 2012.
(27) Adebowale, K. O.; Unuabonah, E. I.; Olu-Owolabi, B. I. Adsorption of some heavy metal ions on sulfate- and phosphate-modified Kaolin. *Appl. Clay Sci.* **2005**, *29*, 145−148.
(28) Kinniburgh, D. G.; Jackson, M. L.; Syers, J. K. Adsorption of alkaline earth, transition and heavy metal cations by hydrous oxide gels of Fe and Al. *Soil Sci. Soc. Am. J.* **1976**, *40*, 796−779.
(29) Thomas, H. C. Heterogeneous ion exchange in a flowing system. *J. Am. Chem. Soc.* **1944**, *66*, 1664−1466.
(30) Spence, A.; Kelleher, B. P. FT-IR spectroscopic analysis of kaolinite-microbial interactions. *Vib. Spectrosc.* **2012**, *61*, 151−155.
(31) Socrates, G. *Infrared and Raman Characteristic Group Frequencies*; John Wiley: New York, 2001.
(32) Viera, R. G. P.; Filho, G. R.; de Assuncao, R. M. N.; Meireles, C. S.; Vieira, J. G.; de Oliveira, G. S. Synthesis and characterization of methylcellulose from sugar cane bagasse cellulose. *Carbohydr. Polym.* **2007**, *67* (2), 182−189.
(33) Johston, C. T.; Agnew, S. F.; Bish, D. L. Polarized single crystal Fourier-transform infrared microscopy of Ouray dickite and Keokuk kaolinite. *Clays Clay Miner.* **1990**, *38*, 573−583.
(34) Schroeder, P. A. Infrared Spectroscopy in Clay Science. In *Teaching Clay Science*; Rule, A., Guggenheim, S., Eds.; The Clay Mineral Society: Chantilly, VA, 2002; Vol. *11*, pp 181−206.
(35) Frost, R. L.; Vassallo, A. M. The dehydroxylation of the kaolinite clay minerals using Infrared emission spectroscopy. *Clays Clay Miner.* **1996**, *44* (5), 635−651.
(36) Unuabonah, E. I.; Adebowale, K. O.; Olu-Owolabi, B. I. Kinetic and Thermodynamic studies of the adsorption of lead (II) ions onto phosphate-modified kaolinite clay. *J. Hazard. Mater.* **2007**, *144*, 386−395.
(37) Farmer, V. C.; Russell, J. D. The Infrared spectra of layered silicates. *Spectrochem. Acta* **1964**, *20*, 1149−1173.
(38) Saika, B. J.; Parthasarathy, G. Fourier Transform Infrared Spectroscopic Characterization of Kaolinite from Assam and Meghalaya, Northeastern India. *J. Mod. Phys.* **2010**, *1*, 206−210.
(39) Madejova, J. FTIR techniques in clay mineral studies. *Vib. Spectrosc.* **2003**, *31*, 1−10.
(40) Moore, D. M.; Reynolds, R. C., Jr. *X-ray Diffraction and the Identification and Analysis of Clay Minerals*; Oxford University Press: Cambridge, U.K., 1989.
(41) Michaelian, K. H.; Bukka, K.; Permann, D. N. S. Photoaccoustic infrared spectra (250−10,000 cm^{-1}) of partially deuteriated kaolinite. *Can. J. Chem.* **1987**, *65*, 1420−1423.
(42) Rivera-Utrilla, J.; Sánchez-Polo, M. Adsorption of Cr(III) on ozonised activated carbon. Importance of Cπ—cation interactions. *Water Res.* **2003**, *37* (14), 3335−3340.
(43) *Bentonite, Kaolin and Selected Clay Minerals*; Environmental Health Criteria 231; WHO: Geneva, 2005.
(44) Yilmaz, G. The effects of temperature on the characteristics of kaolinite and bentonite. *Sci. Res. Essays* **2011**, *6* (9), 1928−1939.
(45) Luangkiattikhum, P.; Tangsathitkulchai, C.; Tangsathitkulchai, M. Non-isothermal thermogravimetric analysis of oil palm solid wastes. *Bioresour. Technol.* **2008**, *99*, 986−997.
(46) Font, R.; Marcilla, A.; Garcia, A. N.; Caballero, J. A.; Conesa, J. A. Kinetic models for the thermal degradation of heterogeneous materials. *J. Anal. Appl.Pyrolysis* **1995**, *32*, 29−39.
(47) Lupascu, T.; Dranca, I.; Popa, V. T.; Vass, M. Application of thermal analysis to the study of some waste agricultural products for the preparation of active carbon. *J. Therm. Anal. Calorim.* **2001**, *63*, 855−863.
(48) Kandiyoti, R.; Herod, A.; Bartle, K. *Solid Fuels and Heavy Hydrocarbon Liquids: Thermal Characterization and Analysis*; Elsevier: London, 2006.
(49) Puangsri, T.; Abdulkarim, S. M.; Ghazali, H. M. Properties of *Carica papaya* L (papaya) seed oil following extraction using solvent and aqueous enzymatic methods. *J. Food Lipids* **2005**, *12*, 62−76.
(50) Sutcu, H.; Piskin, S. The pyrolytic characteristics and kinetics of agricultural waste, bituminous coal, and their blends. *Mater. Manuf. Processes* **2011**, *26*, 99−103.
(51) Miller, B. G.; Tillman, D. A. *Combustion Engineering Issues for Solid Fuel Systems*; Elsevier: Burlington, MA, 2008.
(52) Guidelines for Drinking Water Quality, 4th ed.; WHO: Geneva, 2011. www.who.int/water_sanitation_health/publications/2011/dwq_chapters/en/index.html (accessed May 11, 2013).
(53) Mobasherpour, I.; Salahi, E.; Pazouki, M. Comparative of the removal of Pb^{2+}, Cd^{2+} and Ni^{2+} by nanocrystallite hydroxyapatite from aqueous solutions: Adsorption isotherm study. *Arabian J. Chem.* **2012**, *5*, 439−446.